Spatial correlation of conduction electrons in a metal with a complicated geometry of the Fermi surface

1993 J. Phys.: Condens. Matter 5 1481

(http://iopscience.iop.org/0953-8984/5/10/006)

J. Phys.: Condens. Matter 5 (1993) 1481–1492. Printed in the UK

Spatial correlation of conduction electrons in a metal with a complicated geometry of the Fermi surface

D I Golosov† and M I Kaganov

P L Kapitza Institute for Physical Problems, Russian Academy of Sciences, Vorobyovskoye Chaussée 2, Moscow 117334, Russia

Received 6 March 1992, in final form 9 November 1992

Abstract. The 'density–density' correlation function (CF) of conduction electrons in a metal is investigated. It is shown that the asymptotic behaviour of the CF depends on the shape and the local geometry of the Fermi surface (FS). In particular, the exponent of the power law which describes the damping of Friedel oscillations at $r \to \infty$ (-4 for an isotropic Fermi gas) is determined by the local geometry of the FS. The applications of the results obtained to calculations of the CF in a metal near the electron topological transition and of the RKKY exchange integral are considered as well.

1. Introduction

In this paper we investigate the 'density–density' correlation function (CF) of conduction electrons in a metal at $T = 0$.

It is well known that the CF of an electron gas can be written as

$$\nu(\boldsymbol{r}) \equiv \frac{1}{\overline{n}}\langle \Delta n(\boldsymbol{r}_1)\, \Delta n(\boldsymbol{r}_2)\rangle - \delta(\boldsymbol{r}_1 - \boldsymbol{r}_2) = -\frac{2}{\overline{n}}\left|\int n_{\boldsymbol{p}} \exp\left(\frac{i\boldsymbol{p}\cdot\boldsymbol{r}}{\hbar}\right)\frac{\mathrm{d}^3 p}{(2\pi\hbar)^3}\right|^2 \qquad (1)$$

$\boldsymbol{r} = \boldsymbol{r}_2 - \boldsymbol{r}_1$.

Here the angular brackets indicate the average, $\Delta n(\boldsymbol{r}) = n(\boldsymbol{r}) - \overline{n}$ is the departure of electron density $n(\boldsymbol{r})$ from its average value $\overline{n}$,

$$n_{\boldsymbol{p}} = \begin{cases} 1 & \epsilon(\boldsymbol{p}) < \epsilon_{\mathrm{F}} \\ 0 & \epsilon(\boldsymbol{p}) > \epsilon_{\mathrm{F}} \end{cases} \qquad (2)$$

is the Fermi distribution function, $\boldsymbol{p}$ is the momentum and ϵ_{F} is the Fermi energy. Note that equation (1) is valid for any (not necessarily isotropic) dispersion law $\epsilon(\boldsymbol{p})$.

Let us recall that, for $\epsilon(\boldsymbol{p}) = p^2/2m$, equation (1) leads to the following expression for the CF [1]:

$$\nu(\boldsymbol{r}) \simeq (3\hbar/2\pi^2 p_{\mathrm{F}} r^4)\cos^2(p_{\mathrm{F}} r/\hbar) \qquad r \gg \hbar/p_{\mathrm{F}} \qquad (3)$$

(p_{F} is the Fermi momentum), which contains Friedel oscillations (FOs) [2] with the wavenumber $2p_{\mathrm{F}}/\hbar$.

† Also at: Department of Physics, Rutgers University, Piscataway, NJ 08855-0849, USA.

0953-8984/93/101481+12$07.50

One can easily determine the wavenumbers of the FOs (if the direction of the radius vector $\boldsymbol{r}$ is given) also in the case of an arbitrary dispersion law. Indeed, the long-wavelength behaviour of the CF (equation (1)) is determined by the singularities of the integral given by

$$S(p_\parallel) = \int n_{\boldsymbol{p}}\, \mathrm{d}^2 p_\perp \qquad p_\parallel = \frac{\boldsymbol{p}\cdot\boldsymbol{r}}{r} \qquad \boldsymbol{p}_\perp = \boldsymbol{p} - \frac{p_\parallel \boldsymbol{r}}{r} \tag{4}$$

as a function of $p_\parallel$. Obviously, $S(p_\parallel)$ is simply the square of the section of the Fermi surface (FS) formed by a plane perpendicular to the vector $\boldsymbol{p}$ and located at the distance $p_\parallel$ from the origin in $\boldsymbol{p}$-space. Therefore, the singularities that we are interested in correspond to the tangencies of the FS to planes perpendicular to $\boldsymbol{r}$. The nature of these singularities depends on the *local* geometry of the FS near the points of tangency.

Therefore the wavenumbers Δk_{ij} of the FOs are the distances in $\boldsymbol{p}$-space between planes tangent to the FS and perpendicular to $\boldsymbol{r}$ (figure 1). It is well known that the wavenumbers Δk_{ij} also correspond to the Migdal–Kohn [3] singularities in the spectrum of phonons propagating in the direction $\boldsymbol{r}/r$, as well as to singularities in the longitudinal plasmon spectrum (cf [4]), etc†. Thus, the vectors $\Delta k_{ij}\,\boldsymbol{r}/r$ define the distinct points in the *reciprocal* space; since the present paper is devoted to the spatial correlation of electrons, we shall study the effects that occur in the *real* space.

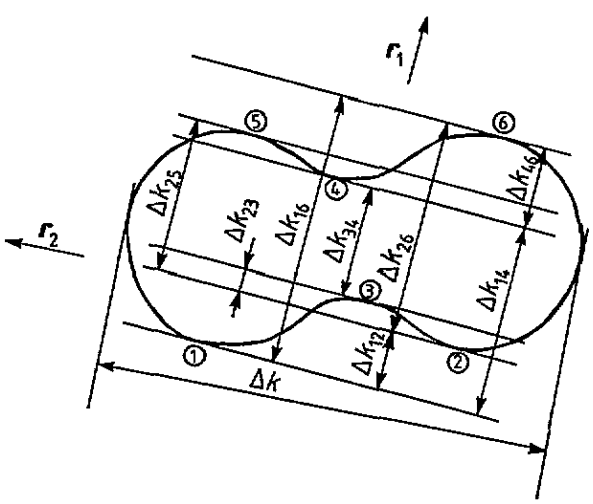

Figure 1. Rather a simple FS ('dumb-bell') for the radius vector $\boldsymbol{r}\|\boldsymbol{r}_1$ generates eight different wavenumbers of FOs (owing to the symmetry, $\Delta k_{12} = \Delta k_{56}$, $\Delta k_{13} = \Delta k_{46}$, $\Delta k_{14} = \Delta k_{25} = \Delta k_{36}$, $\Delta k_{15} = \Delta k_{26}$, $\Delta k_{23} = \Delta k_{45}$ and $\Delta k_{24} = \Delta k_{35}$). The encircled numbers enumerate the points of tangency for this case. The total number of wavenumbers depends on the direction of $\boldsymbol{r}$; for $\boldsymbol{r}\|\boldsymbol{r}_2$ there is only the wavenumber Δk.

† Also, the quantities $(\Delta k_{ij})^{-1}$ are proportional to the periods of oscillation of the sound absorption coefficient in a magnetic field [5].

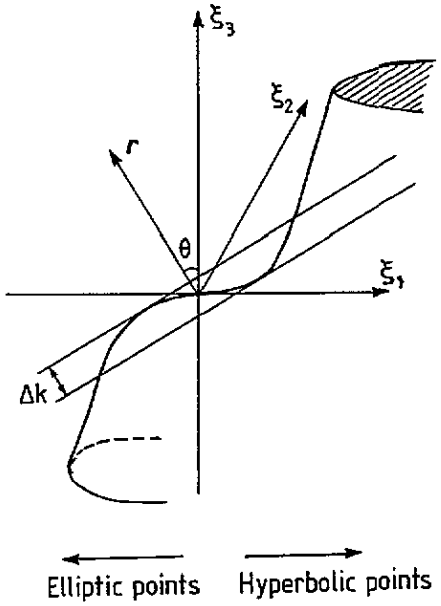

Figure 2. Parabolic point on the FS (placed at the origin of local coordinates ξ_1, ξ_2, ξ_3, where ξ_3 is parallel to the normal). For a small value of the angle $\theta > 0$, there are two points of tangency in the vicinity of the parabolic point: elliptic (with $\xi_1 < 0$) and hyperbolic (with $\xi_1 > 0$) and, correspondingly, the small wavenumber $\Delta k \propto \theta^{3/2}$. As $\theta \to +0$, these points of tangency approach each other; at $\theta = 0$, they coincide at the parabolic point; at $\theta < 0$, there are no points of tangency in the vicinity of this parabolic point (see also figure 3(*a*)).

One can also come to the same conclusions if one considers the Fourier component of the CF given by

$$\nu(\boldsymbol{k}) = -\frac{2}{\overline{n}} \int n_{\boldsymbol{p}} n_{\boldsymbol{p}+\hbar\boldsymbol{k}} \frac{\mathrm{d}^3 p}{(2\pi\hbar)^3} \tag{5}$$

which is proportional to the volume of the intersection of the FS and its analogue, shifted by the vector $\hbar\boldsymbol{k}$. The singularities of this quantity (as a function of $\boldsymbol{k}$) correspond to the tangents of the FS to its shifted analogue, as well as to $\boldsymbol{k} = \boldsymbol{0}$. We may conclude tentatively (see section 2 below) that the way in which FOs are damped at $r \to \infty$ is determined by the local geometry of the FS at the points of tangency. Thus, the behaviour of the CF, as well as of many other electronic properties of metals [6], is determined by the FS geometry.

It turns out that one can describe the asymptotic behaviour of the CF at large r by the formula

$$\nu(r) = -\frac{1}{32\pi^4} \frac{r_e^3}{r^4} \sum_{ij} A_i^* A_j \exp(\mathrm{i}\Delta k_{ij} r). \tag{6}$$

Here $r_e = \overline{n}^{-1/3}$ is the average distance between electrons, and the indexes i, j label the points of tangency. The factors A_i (which are, in general, functions of r as well

as of r/r) depend on the local geometry of the FS at the corresponding points of tangency and have a dimensionality of inverse length. Owing to the central symmetry of the FS, expression (6) is real (obviously, $\Delta k_{ij} = -\Delta k_{ji}$).

At $i = j$, $\Delta k_{ij} = 0$ and the corresponding terms in the CF decrease monotonically as r increase. These terms are due to the singularity (namely, the discontinuity of the first derivative) of $\nu(k)$ at $k = 0$.

Usually, one can write the validity condition for equation (6) as $\Delta k_{ij}\, r \gg 1$ for any $i \neq j$. Note that the wavenumbers Δk_{ij} (as well as their total number) depend on the direction of the radius vector r.

So far we have discussed the electron gas with an arbitrary dispersion law. The coordinate dependence of the CF of conduction electrons in a real metal is not totally covered by equation (1). In order to describe this case, one should take into account the influence of the periodic potential of the crystal lattice not only on the spectrum but also on the electron wavefunctions; the wavefunctions that should now be used are the Bloch waves (instead of plane waves). This topic has been considered in detail in our previous article [7]. The qualitative results of this straightforward although somewhat cumbersome consideration are listed below.

(1) Because of the broken translation invariance, the coordinate dependence of the CF $\nu(r_1, r_2)$ is not reduced to the dependence only on the difference $r = r_2 - r_1$ between its arguments. If the value of r is fixed, $\nu(r_1, r_2)$ is a periodic function of r_1:

$$\nu(r_1, r_2) = \nu(r_1, r + r_1) = \nu(r_1 + a, r + r_1 + a) \tag{7}$$

where a is any lattice period.

(2) Let us keep r = constant and average $\nu(r_1, r_2)$ over r_1. Denote the quantity obtained by $\nu(r)$. Its asymptotic behaviour will be similar to that described by equation (6). The wavenumbers of the FOS are to be determined in the same way; the only difference is that now one should imagine the FS as a periodic surface in the reciprocal space (and not restricted to the first Brillouin zone alone!). Therefore, the expression for $\nu(r)$ should contain a summation over the reciprocal-lattice vector b; terms with $b \neq 0$ (*Umklapp* terms) oscillate with a wavenumber $\Delta k_{ij} + b \cdot r/r$.

(3) The CF contains a term whose oscillation wavelength is the inverse diameter of the FS. Note, however, that if the FS is open, a region of radius vector r directions can exist in which $\nu(r)$ does not oscillate at all.

Let us now consider the dependence of the CF on the local geometry of the FS. For simplicity, we shall restrict ourselves to the analysis of equations (1) and (6); this approach may be easily generalized for the case of conduction electrons in a real metal [7].

2. The effect of the local geometry of the Fermi surface on the correlation function

From equation (6), it follows that each term in the CF contains the factors A_i, which depend on the local geometry of the FS at each of the two contributing points of tangency. The expressions for $A_i(r)$ for various cases are listed below. We shall not describe the calculations here; this type of description can be found in [7].

Let us keep the direction of the radius vector r fixed and consider the factor A_i, corresponding to the ith point of tangency.

(i) If it is an elliptic point, then

$$A_{\text{ell}} = 2G^{-1/2} \tag{8}$$

where G is the Gaussian curvature (product of the principal curvatures [8]) of the FS.

(ii) For a hyperbolic point of tangency, one obtains

$$A_{\text{hyp}} = \pm 2\mathrm{i}|G|^{-1/2} \tag{9}$$

where the sign depends on the direction of the radius vector (i.e. whether it is $\boldsymbol{r}$ or $-\boldsymbol{r}$).

In these cases, A does not depend on r, and the amplitude of the FOs corresponding to a pair of elliptic and/or hyperbolic points of tangency decreases at $r \to \infty$ as r^{-4}.

(iii) The domains of elliptic and hyperbolic points on the FS are separated by lines of *parabolic* points. Apart from a very few exceptions (Na, K, Cs, Rb and Bi), the FSs of real metals are rather complex and do contain the lines of parabolic points [6, 9].

In the generic case, one can choose the local coordinates ξ_1, ξ_2 on the FS in such a way that the departure ξ_3 of the FS from the plane, which is a tangent at a parabolic point, is

$$\xi_3(\xi_1, \xi_2) \simeq C\xi_1^3 - B\xi_2^2 \tag{10}$$

(here we restrict ourselves to the leading order in x, y). We shall assume, for convenience, that $B > 0$ and $C > 0$.

If the point of tangency is parabolic, then

$$A_{\text{par}} \simeq \left\{2\mathcal{K}[\sin(\pi/12)]\Gamma(\tfrac{5}{6})/(3^{1/4}C^{1/3}B^{1/2}\pi)\right\} r^{1/6} \propto r^{1/6}. \tag{11}$$

Here $\mathcal{K}$ is the elliptic integral, Γ is Euler's gamma function and $\mathcal{K}[\sin(\pi/12)]\Gamma(\frac{5}{6}) \simeq 1.5$.

Thus we immediately see that, if parabolic points of tangency appear at a given direction of $\boldsymbol{r}$, then the amplitude of the corresponding term in the CF decreases as $r^{-11/3}$, i.e. slower than in the usual case. Because parabolic points on the FS are not isolated but form continuous lines, there exist cones of radius vector directions corresponding to the presence of parabolic points of tangency.†

Let us now denote by $\Delta\theta$ the angle between the normal at the parabolic point and the projection of the radius vector onto the plane perpendicular to the line of parabolic points (figure 2). At $\Delta\theta < 0$, there are no points of tangency near the parabolic points. At $\Delta\theta > 0$, however, both elliptic and hyperbolic points of tangency exist and both approach a parabolic point as $\Delta\theta \to 0$. Therefore in the CF there appears an additional long-wavelength term which has the wavenumber

$$2 \times 3^{-3/2}C^{-1/2}(\Delta\theta)^{3/2}.$$

† If the FS contains parabolic points, then the singularities of kinetic characteristics of the metal are enhanced for the corresponding directions of the quasi-momentum vector [10, 11].

Because of the vicinity of a parabolic point, equations (8) and (9) should be modified (one may not take into account the terms quadratic in x, y only). Thus, for an elliptic point (figure 2, $x < 0$), we have

$$A_{\text{ell}} \simeq B^{-1/2}(3C\,\Delta\theta)^{-1/4}\left\{1 - [5\mathrm{i}C^{1/2}/16 \times 3^{1/2}\,(\Delta\theta)^{3/2}](1/r)\right\} \tag{12}$$

and, for a hyperbolic point, we have

$$A_{\text{hyp}} \simeq \mathrm{i}B^{-1/2}(3C\,\Delta\theta)^{-1/4}\{1 + [C^{1/2}/2\pi 3^{1/2}(\Delta\theta)^{3/2}][1 - (5\pi/8)\mathrm{i}](1/r)\}. \tag{13}$$

This distinction between elliptic and hyperbolic points is not so surprising. One has to remember that the singularities of $\nu(k)$ corresponding to elliptic and hyperbolic points of tangency are somewhat different.

Both equation (12) and equation (13) are valid at

$$\Delta\theta \gg (r^2/C)^{1/3}. \tag{14}$$

Suppose that at $\Delta\theta < 0$ there exist $2\mathcal{N}$ points of tangency (here we are taking into account the symmetry of the FS) and, therefore,

$$2\mathcal{N} - 1 + \mathcal{N}(\mathcal{N} - 1)/2 = \mathcal{N}(\mathcal{N} + 3)/2 - 1$$

different wavenumbers of FOS. At $\Delta\theta = 0$ there appear two new (parabolic) points of tangency, and the amount of FO wavenumbers increases by $\mathcal{N} + 2$. Then, at $0 < \Delta\theta \lesssim (r^2/C)^{1/3}$, the crossover occurs (the contribution of each parabolic point of tangency turns into the sum of contributions of elliptic and hyperbolic points of tangency) and finally at $\Delta\theta \gg (r^2/C)^{1/3}$ there are $2(\mathcal{N}+2)$ points of tangency and

$$(\mathcal{N} + 2)(\mathcal{N} + 5)/2 - 1$$

FO wavenumbers.

Let us consider the Gauss map of the FS (figure 3(a)). The Gauss map is a mapping of the surface onto the unit sphere, induced by the normal at each point of the surface (the direction of the normal gives a point of the sphere, thus giving the image of an original point of the surface) [8]. The number of points of tangency changes by 4 as the point, which represents the direction of the radius vector, crosses the line corresponding to the directions of the normals at parabolic points. This is the only way for this number to be changed. Suppose that for the direction of a radius vector lying within the area 1 (see figure 3(a)) the total number of points of tangency (on the whole FS) is $2\mathcal{N}$. Then for $\boldsymbol{r}/r$ situated on the lines BE or ED there are $2(\mathcal{N} + 1)$ points of tangency (two parabolic points have been added). The number of points of tangency for $\boldsymbol{r}/r$ lying in areas 2 and 4, on lines AE or EC, and in area 3 are given by $2(\mathcal{N} + 2)$, $2(\mathcal{N} + 3)$ and $2(\mathcal{N} + 4)$, respectively. The angle θ appearing in figure 2 is just the distance between the point $\boldsymbol{r}/r$ and the image of the line of parabolic points on the Gauss map.

(iv) Points at which the FS becomes flat [12] manifest another type of local geometry. The FS with such a point is a boundary case between convex surfaces and surfaces with a 'crater'. Near this flattening point, the departure of the FS from

the tangent plane is a fourth-order form of the local coordinates within the surface. If the point of tangency is a point of such a kind, then

$$A_{\text{fl}} \propto r^{1/2}. \tag{15}$$

Let us assume for definiteness that the departure of the FS from the plane tangent to the FS at the flattening point is given in the leading order by

$$\xi_3(\xi_1, \xi_2) \simeq D(\xi_1^2 + \xi_2^2)^2 = D\xi_\perp^4. \tag{16}$$

Then, as the (elliptic) point of tangency approaches the flattening point, the Gaussian curvature decreases and

$$A_{\text{ell}} \approx 2^{5/6} 3^{-1/2} D^{-1/3} \Delta\theta^{-2/3}. \tag{17}$$

Here $\Delta\theta$ is now the angle between the radius vector and the normal to the FS at the flattening point. Equation (17) is valid at

$$\Delta\theta \gg D^{1/4} r^{-3/4} \tag{18}$$

where the intermediate region is the region of crossover between the dependences (15) and (17) (see figure 3(*b*)).

(v) Suppose that the lines of parabolic points on the FS cross at some point. In real metals, such a crossing occurs rather often; for example, the FS of the form shown in figure 4 is encountered in Mo, W and paramagnetic Cr [6, 9, 11].

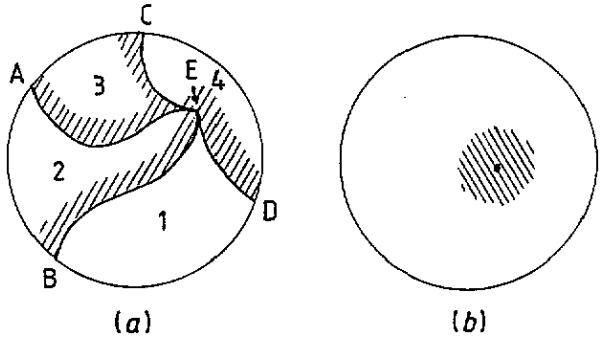

Figure 3. Gauss maps of elements of the FS. (*a*) The image of part of the FS with two lines of parabolic points AC and BD intersecting at the point E. Each point in areas 2 and 4 is the image of the two points from the original part of the FS; each point in area 3 is the image of four points; each point in area 1 does not have any original there. The shaded areas correspond to crossover (the inequality (14) is broken there). This obviously is only one of the two kinds of intersection of the lines of parabolic points. (*b*) Gauss map of the part of the FS containing the point at which the FS becomes flat. The number of points of tangency is constant for r/r lying in this region of directions. The shaded area corresponds to crossover (inequality (18) is broken there).

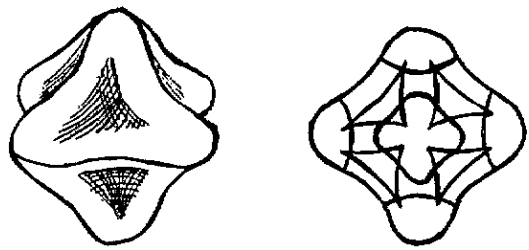

(*a*) (*b*)

Figure 4. Crossing of the lines of parabolic points on the FS [11]: (*a*) fragment of the FS ('octahedron') in a metal belonging to the molybdenum group; (*b*) crossing of lines of parabolic points on this cavity of the FS (view from above).

The departure of the FS from the plane tangent to the FS at this point of crossing is given by a third-order form and we have

$$A_{\text{or}} \propto r^{1/3}. \tag{19}$$

In fact, this is a flattening point of another kind. The important feature of flattening points of tangency of any type is that they correspond to isolated points on the Gauss map (see figure 3).

(vi) Let us assume that the FS contains finite flat elements. If the radius vector is parallel to the normal to such an element of the FS, it leads to the contribution of this 'area of tangency' in the CF:

$$A_{\text{plane}} \propto S_{\text{plane}} r \tag{20}$$

where S_{plane} is the square of this flat element.

In fact, the FS of such a kind can hardly be stable: in this case, the Peierls [13] transition with the transformation of the lattice strucure should become energetically favourable (at least at sufficiently low temperatures). It is easy to see that there should be some correlation between the extremely slow damping of FOs as $r \to \infty$ (here $\nu \propto r^{-2}\cos(\Delta k_{\text{plane}}\, r)$) and the possibility of the Peierls transition.

At this point we finish our consideration of the local geometry of the FS. Note that we have arrived at the remarkable conclusion that the exponent, which determines the damping of FOs as $r \to \infty$, depends on the local geometry at the points of tangency. Thus, one might build up a hierarchy of types of the FS local geometry with respect to the long-distance behaviour of the CF.

(1) *Spherical FS.* The amplitude of the FOs decreases as r^{-4}; this exponent is given, generally, by elliptic or hyperbolic points of tangency and thus corresponds to a generic direction in a 3D metal.

(2) *Cylindrical FS.* The amplitude of the FOs decreases as r^{-3}. This is the case of a 2D metal, or the case of a toroidal FS cavity (see section 5 of [7])†.

(3) *Flat FS.* The amplitude of the FOs decreases as r^{-2} (one could imagine it as a FS of a 1D metal).

From our considerations, it follows that parabolic points (together with crossing points of the lines of parabolic points) should be placed 'between' spherical and cylindrical FSs.

† The point at which the FS becomes flat also gives the r^{-3} law (see equation (15)).

3. Some applications

Let us consider a metal near the electron topological transition (ETT) point [14]. The ETT is the restructuring of the FS which occurs when $\epsilon_F = \epsilon_{cr}$ (ϵ_{cr} is the value of the electron energy that corresponds to the Van Hove singularity). Depending on whether this singularity is due to an extremum or to a saddle point of the electron dispersion law, a new cavity of the FS appears (disappears), or a 'neck' connecting two FS cavities is formed (disrupted). The difference $z = \epsilon_F - \epsilon_{cr}$ depends on the applied pressure (or, for example, the impurity concentration), so that the ETT can be realized experimentally (see [15] and references therein). The ETT causes distinctive singularities of thermodynamic and kinetic quantities [14–16].

Near the ETT point, long-wavelength terms appear in the CF owing to the existence of small diameters of the FS. If the ETT results in the appearance of a new cavity of the FS at $z > 0$, then

$$\nu_{ETT}(r) \simeq -\frac{4}{\overline{n}\pi^4}\frac{z}{\hbar^2}\left(m_1m_2m_3\Big/ r^4\sum_{i=1}^{3}(m_i\cos^2\theta_i)\right) \times \cos^2\left[\left(2zr\sum_{i=1}^{3}m_i\cos^2\theta_i\right)^{1/2}\Big/\hbar\right]. \tag{21}$$

Here m_1, m_2 and m_3 are effective masses and the axes $\hat{x}_1$, $\hat{x}_2$ and $\hat{x}_3$ (where $x_i = r\cos\theta_i$) are the main axes of the tensor of inverse effective masses, so that the electron dispersion law near the point of extremum can be written as

$$z \simeq (\Delta p_1)^2/2m_1 + (\Delta p_2)^2/2m_2 + (\Delta p_3)^2/2m_3. \tag{22}$$

If (instead of an extremum) one has a saddle point of the dispersion law, one should write, instead of (22),

$$z \simeq [(\Delta p_1)^2 + (\Delta p_2)^2]/2m_\perp - (\Delta p_3)^2/2m_\parallel + (\beta/4m_\parallel^2)(\Delta p_3)^4 \tag{23}$$

(we assume that the FS near the extremal point $\Delta p = 0$ possesses rotational symmetry with respect to the p_3 axis and is also symmetric with respect to the $\Delta p_3 = 0$ plane). In this case, the 'neck' of the FS, which exists at $z > 0$, is ruptured at $z < 0$ (figure 5). Therefore, at $|z| \ll \epsilon_F$ there exist long-wavelength ($\Delta k \lesssim (2m|z|)^{1/2}/\hbar \ll k_F$) terms in the CF. The issue of significance here is that the angular dependence of these terms 'rotates' by $\pi/2$ as the sign of z changes.

Indeed, for example, at $z < 0$ and $r \| p_3$, because of the small distance between the two sheets of the FS, there exists a long-wavelength component of the FOs with corresponding $\Delta k = (2m_\parallel|z|)^{1/2}/\hbar$ and amplitude $m_\perp^2|z|r^{-4}/2\hbar^2\pi^4\overline{n}m_\parallel$. There are no long-wavelength oscillations at $r \perp p_3$. On the contrary, for $z > 0$, the long-wavelength oscillations are absent at $r \| p_3$. For $z > 0$ and $r \perp p_3$, owing to the small diameter of the FS 'neck', the following long-wavelength term in the CF appears:

$$\nu_{ETT}(r)\big|_{r\perp p_3} \simeq -(m_\parallel z/\pi^4\overline{n}r^4\hbar^2)\sin^2[r(2m_\perp z)^{1/2}].$$

At $\beta z > 0$, the fourth-order term in (23) gives rise to the appearance of lines of parabolic points on the FS near $p = p_{cr}$ [16]† (see figure 5). Thus, for some directions

† Note that parabolic points on the FS themselves are not peculiar from the viewpoint of the electron dispersion law. Generally, the lines of parabolic points may have nothing to do with ETT or Van Hove singularities (see section 2 above).

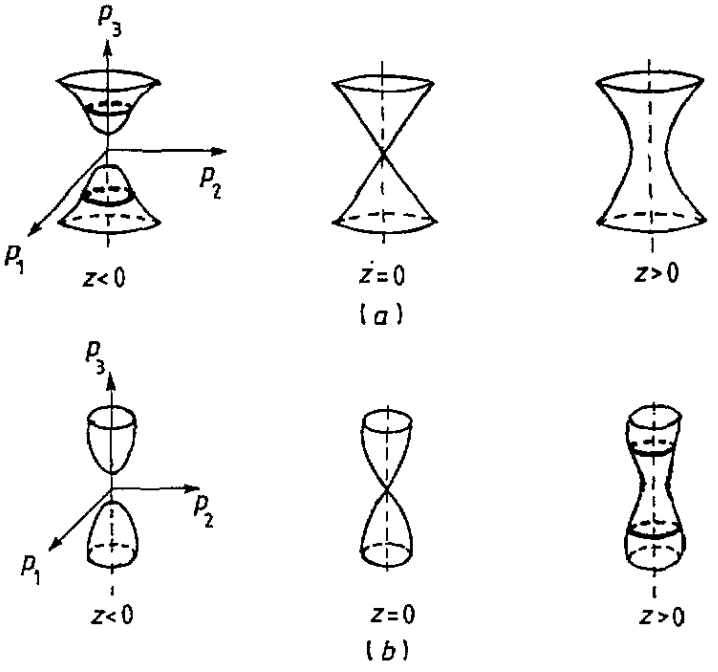

Figure 5. (*a*) Disappearance and (*b*) appearance of the lines of parabolic points (indicated as bold lines) during the 'neck' formation [16].

of r forming an angle θ_{par} with the p_3 axis, the amplitude of the long-wavelength term in the CF behaves as $r^{-11/3} = r^{-4}r^{2/3}$ instead of r^{-4}. In the neighbourhood of these peculiar directions, there exists an additional small wavenumber of FOs, which is due to neighbouring pairs of points of tangency (elliptic and hyperbolic). At $\theta = \theta_{par}$, each pair 'sticks together', giving the parabolic point of tangency and then disappearing.

On the whole, the ETT, being a local 'event' in reciprocal space, in coordinate space results in dramatic restructuring of the long-wavelength terms in the CF.

Obviously, knowledge of the CF is useful when one considers various collective phenomena in metals: screening, structure of spin glasses, etc. Let us mention for example the RKKY interaction [17–19]. This indirect exchange interaction between the site (or impurity) spins is caused by exchange interaction between the localized spins and conduction electrons:

$$\mathcal{H} = \frac{J}{\overline{n}} \sum_i \sigma \cdot \boldsymbol{S}_i \delta(\boldsymbol{r} - \boldsymbol{r}_i). \tag{24}$$

Here J is the exchange constant, σ is the Pauli matrix, and $\boldsymbol{S}_i$ are the spins of the ion located in the site $\boldsymbol{r}_i$. The RKKY exchange integral is

$$J_{\mathrm{RKKY}}(\boldsymbol{r}) = -2\left(\frac{J}{\overline{n}}\right)^2 \int \frac{n_q(1-n_{q'})}{\epsilon(q)-\epsilon(q')} \exp\left(\frac{\mathrm{i}(q-q')\cdot r}{\hbar}\right) \frac{\mathrm{d}^3q\,\mathrm{d}^3q'}{(2\pi\hbar)^6} \tag{25}$$

and its Fourier component

$$J_{\mathrm{RKKY}}(k) = -2\left(\frac{J}{\overline{n}}\right)^2 \int \frac{n_q(1-n_{q-\hbar k})}{\epsilon(q)-\epsilon(q-\hbar k)} \frac{\mathrm{d}^3q}{(2\pi\hbar)^6}. \tag{26}$$

This kind of integral also appears when studying the electron–phonon interaction. It has singularities at the same points as does the CF (except at $k = 0$). These singularities are called Migdal–Kohn [3] singularities if the electron velocity vectors at the two contributing points of tangency are antiparallel. On the other hand, if they are parallel, then the singularity is called a Taylor [20] singularity and these two cases should be treated separately.

It turns out that at least for the great majority of cases there exists a quite simple relationship between the asymptotics of $\nu(r)$ and $J_{\mathrm{RKKY}}(r)$. Indeed, for a fixed direction of the radius vector,

$$J_{\mathrm{RKKY}}^{(\Delta k)} \propto r\nu^{(\Delta k)}(r) \qquad \Delta k \neq 0 \tag{27}$$

where $J_{\mathrm{RKKY}}^{(\Delta k)}$ and $\nu^{(\Delta k)}(r)$ are the terms in J_{RKKY} and the CF respectively, oscillating with the wavenumber Δk.

It is well known that the magnetic order induced by the RKKY interaction (namely the helicity vector) depends on the geometry of the FS [18]. Thus, the helicity vector is expected to be determined by the small diameter of the FS [21]. Therefore knowledge of the FS and the CF seems to allow one to make some predictions about the magnetic arrangement. We expect, in particular, that the ETT may manifest itself in changes in magnetic ordering.

4. Conclusion

In this paper, we neglected the temperature effects, electron scattering and electron–electron interactions. The first two effects lead to the appearance of an exponentially decreasing factor in the CF as $r \to \infty$. The third (i.e. Fermi-liquid interaction) probably leads to the renormalization of the coefficients (see, e.g., [22]).

Anyway, the dependence of the asymptotic behaviour of the CF on the FS geometry (including the local geometry) survives after taking these effects into account. This dependence should affect collective phenomena in metals. Indeed, one has to know the CF to construct theories of alloying, screening, exchange magnetism, etc. We have investigated some features of the CF that seem to be interesting from this point of view. Among them are the following.

(1) Cones of peculiar directions exist, corresponding to the lines of parabolic points on the FS. For these directions of the radius vector, the CF shows some specific features:

(i) the attenuation of FOs is determined by a factor of $r^{-11/3}$ instead of the usual r^{-4} (we doubt whether this small difference has any observable effect),

(ii) the number of FO periods changes as the direction of the radius vector crosses these cones and

(iii) on one side of such a cone, one of the FO periods appears to become large (it goes to infinity as the direction of r approaches the cone).

(2) Isolated peculiar directions exist, which correspond to the crossings of the lines of parabolic points on the FS (flattening points).

(3) The CF is restructured when the ETT occurs.

We have also provided one example showing how an asymptote of the RKKY exchange integral depends on the asymptotic behaviour of the CF.

Acknowledgments

It is a pleasure to thank M Yu Kagan and L P Pitaevsky for fruitful discussions. We are also grateful to A Prakash for assistance in preparing this manuscript for publication.

References

[1] Landau L D and Lifshitz E M 1969 *Statistical Physics* (Reading, MA: Addison-Wesley)
[2] Friedel J 1952 *Phil. Mag.* **43** 153; 1954 *Phil. Mag. Suppl.* **3** 446; 1958 *Nuovo Cimento Suppl.* **7** 287
[3] Migdal A B 1958 *Sov. Phys.–JETP* **7** 996
Kohn W 1959 *Phys. Rev. Lett.* **2** 393
[4] Lifshitz E M and Pitaevski L P 1981 *Physical Kinetics* (Oxford: Pergamon)
[5] Gurevich V L 1960 *Sov. Phys.–JETP* **10** 51
[6] Lifshitz I M, Azbel' M Ya and Kaganov M I 1973 *Electron Theory of Metals* (New York: Consultants Bureau)
[7] Golosov D I and Kaganov M I 1992 *Sov. Phys.–JETP* **74** 186
[8] Dubrovin B A, Fomenko A T and Novikov S P 1992 *Modern Geometry—Methods and Applications* (New York: Springer)
[9] Cracknell A P and Wong K C 1973 *The Fermi Surface* (Oxford: Clarendon)
[10] Avanesyan G T, Kaganov M I and Lisovskaya T Yu 1978 *Sov. Phys.–JETP* **48** 900
[11] Kaganov M I, Kontorovich V M, Lisovskaya T Yu and Stepanov N A 1983 *Sov. Phys.–JETP* **58** 975
[12] Kaganov M I and Lifshitz I M 1979 *Sov. Phys.–Usp.* **22** 904
[13] Peierls R E 1955 *Quantum Theory of Solids* (Oxford: Clarendon)
[14] Lifshitz I M 1960 *Sov. Phys.–JETP* **11** 1130
[15] Varlamov V A, Egorov V S and Pantsulaya A V 1989 *Adv. Phys.* **38** 469
[16] Kaganov M I and Gribkova Yu V 1991 *Sov. J. Low. Temp. Phys.* **17** 473
[17] Ruderman M A and Kittel C 1954 *Phys. Rev.* **96** 99
Kasuya T 1956 *Progr. Theor. Phys.* **16** 45
Yosida K 1957 *Phys. Rev.* **106** 893
[18] Yosida K 1964 *Progress in Low Temperature Physics* vol 4, ed C Corter (Amsterdam: North-Holland) p 265
[19] Abrikosov A A 1988 *Fundamentals of the Theory of Metals* (Amsterdam: North-Holland)
[20] Taylor P L 1963 *Phys. Rev.* **131** 1995
Kaganov M I, Plyavenek A G and Hitschold M 1982 *Sov. Phys.–JETP* **55** 1167
[21] Dzyaloshinskii I E 1965 *Sov. Phys.–JETP* **20** 665
[22] Kaganov M I and Möbius A 1984 *Sov. Phys.–JETP* **59** 405